

## Dynamics of H<sub>2</sub>O and Na<sup>+</sup> in Nafion Membranes

Nick P. Blake, Greg Mills, and Horia Metiu\*

Department of Chemistry & Biochemistry University of California, Santa Barbara California 93106-9510

Received: October 2, 2006; In Final Form: December 19, 2006

We investigate the transport properties of a model of a hydrated Na-Nafion membrane using molecular dynamics simulations. The system consists of several Nafion chains forming a pore with the water and ions inside. At low water content, the hydrophilic domain is not continuous and diffusion is very slow. The diffusion coefficient of both water and Na<sup>+</sup> increases with increasing hydration (more strongly so for Na<sup>+</sup>). The simulations are in qualitative agreement with experimental results for similar systems. The diffusion coefficient is an average over the motion of ions or water molecules located in different environments. To better understand the role of the environment, we calculate the distribution of the residence times of the ion (or water) at different locations in the system. We discuss the transport mechanism in light of this information.

### I. Introduction

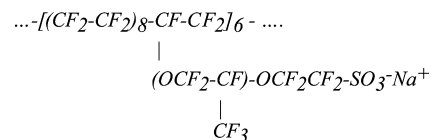
Nafion is a polymer electrolyte membrane (PEM) made of a polytetrafluoroethene (PTFE) polymer with perfluorovinylsulfonic acid side chains. The PTFE backbone is hydrophobic while the acid group on the side chain is hydrophilic. When hydrated, the polymer aggregates to form hydrophobic and hydrophilic domains. Proton conduction, which is very high in this material, takes place through the hydrophilic channels. This, combined with Nafion's excellent resistance to oxidation or reduction, makes it one of the foremost proton conducting polymer membranes for methanol or hydrogen fuel cells.<sup>1–4</sup>

In a recent paper we examined the morphology of Na–Nafion membranes using molecular dynamics simulations.<sup>5</sup> We found that at 5 wt % hydration, the SO<sub>3</sub>Na groups aggregate with the water to form very small droplets (5–8 Å) with several SO<sub>3</sub><sup>–</sup> groups in the first solvation shell of Na<sup>+</sup>. As the amount of water is increased, the membrane swells and SO<sub>3</sub>Na dissociates into ions. The side-chains preferentially line up along the domain wall with the SO<sub>3</sub> groups pointing into the hydrophilic phase. This observation supports qualitatively models in which the negative ions are located on the wall of the domain.<sup>6,7</sup> The swelling is accompanied by a transition to a percolating hydrophilic network consisting of irregular, curvilinear water channels (10–20 Å in cross-section) permeating the membrane in all directions. At the highest loading we have considered (19 wt % water), a water molecule exhibits a much broader distribution of nearest neighbors than expected in liquid water; sometimes we found that a water molecule can have as many as eight water molecules next to it. These findings are consistent with those of other Nafion simulations.<sup>8–14</sup>

In this article, we examine Na<sup>+</sup> and water transport through the sodium salt of Nafion. We do not consider proton transport since this requires special potential energies, including quantum effects.<sup>15–19</sup> Our main concern here is the manner in which mobility is shaped by the morphology and by the degree of hydration of the membrane.

### II. Simulation Details

We model the Nafion membrane using molecular dynamics with an AMBER FF02EP force-field<sup>20</sup> and the partial charge scheme of Vishnyakov and Neimark.<sup>10</sup> To mimic the macroscopic membrane we place 12 Nafion strands (Nafion-1166)



within an orthorhombic cell with variable amounts of TIP4P water<sup>21</sup> and subject the contents to periodic boundary conditions. Charge–charge interactions are modeled by using Ewald sums for the infinite periodic array of orthorhombic cells. Bond lengths are constrained using the SHAKE algorithm,<sup>22</sup> allowing us to take femtosecond time steps even though vibrating H atoms are present in the system. The water loadings we examine are 5, 7, and 19 wt % water; which correspond to 3.4, 7.3, and 14.5 waters per SO<sub>3</sub> group; there are 72 SO<sub>3</sub> groups and the number of water molecules is 244, 524, and 1044, respectively. Other details regarding system preparation are given in our previous paper.<sup>5</sup>

To characterize the transport properties of the system we calculate self-diffusion coefficients according to the Einstein formula,

$$D = \lim_{t \rightarrow \infty} \frac{\langle \Delta R_{cm}(t)^2 \rangle}{6t} \quad (1)$$

The angular brackets denote an equilibrium ensemble average, and the vector  $R_{cm}(t)$  gives the position of the center of mass for the species of interest (Na<sup>+</sup> or H<sub>2</sub>O). If  $D$  is evaluated by performing the average over all the molecules (or ions) in the system, we obtain a global diffusion coefficient. This is what would be measured in an experiment monitoring the ion or water flux across the membrane. However, this system is highly inhomogeneous and a “global” average hides much of the dynamics. Because of this, we also examine the local properties of the system by calculating a histogram of the residence time of a water molecule or an ion in a given local environment.

\* Corresponding author phone: 805.893.2256; fax: 805.893.4120; e-mail: metiu@chem.ucsb.edu.

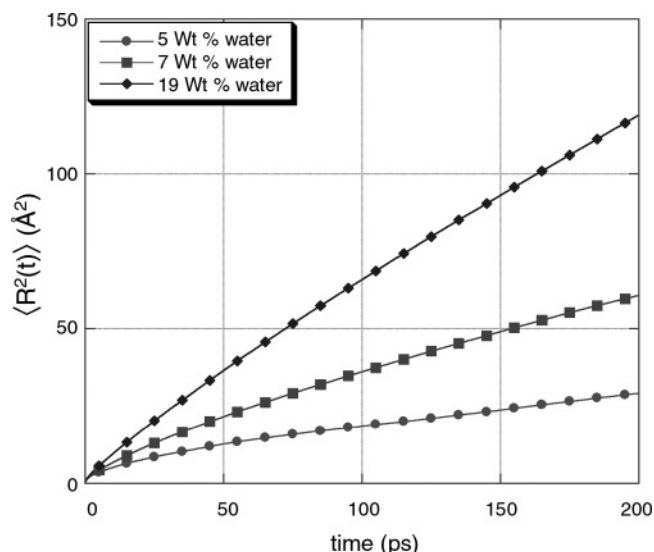


**Figure 1.** Mean-squared displacements of water in three Nafion-1166 membranes: one with a 19 wt % water content, one with a 7 wt % water content, and one with a 5 wt % water content. The diffusion coefficients are  $9.10 \times 10^{-10}$  m<sup>2</sup>/s,  $4.30 \times 10^{-10}$  m<sup>2</sup>/s, and  $1.76 \times 10^{-10}$  m<sup>2</sup>/s, respectively (using only data from after the onset of approximate linearity,  $t > 50$  ps).

For this we divide the space in micro-regions and determine the probability  $\tau_{\alpha j}(t)dt$  that the species  $\alpha$  that was located in a region  $j$  at time zero, leaves it at a time between  $t$  and  $t + dt$ .

We distinguish two processes that can contribute to the residence time. Because our hydrophilic domain is a liquid and the potential binding the particle in a certain region may not be deep, it is possible to have particles that crisscross the region boundary, early and often. These contribute to  $\tau_{\alpha j}(t)$  at short times. To display this behavior, we collect the histogram of  $\tau_{\alpha j}(t)$  in bins of logarithmically increasing width, and plot it against  $\log(t)$ . This “stretches” the time scale for short times and compresses it for long times.

If the process by which a particle leaves a certain region is governed by a first-order rate equation, the residence time distribution will have the form

$$\tau(t) = k \exp(-kt) \quad (2)$$

where  $k$  is the rate constant (the reciprocal of the mean residence time). We find that this is not the case in the system examined here.

### III. Results

**III.1. Global Diffusion.** The mean square displacements of H<sub>2</sub>O (Figure 1), and Na<sup>+</sup> (Figure 2) show a transition from faster quasi-diffusive motion at short times to slower diffusion at longer times. This is expected in any system where motion is hindered by traps. The curves in Figures 1 and 2 have become almost linear at  $t > 50$  ps, although the system with 5 wt % water continues to show trapping effects beyond  $t = 200$  ps, meaning that the reported diffusion coefficient is overestimated.

For the 7 and 19 wt % water systems, the diffusion coefficient at longer times is approximately  $1/3$  that of its  $t = 0$  limit. This is consistent with a transition from a three-dimensional diffusion at short times, to effectively one-dimensional diffusion as the diffuser starts to sample the nonuniformity of the hydrophilic phase and finds that diffusion is only possible along the channel.

To better understand this transition we experimented with three simplified models to test the validity of this interpretation. Each contains one particle hopping on a 2D lattice. The first

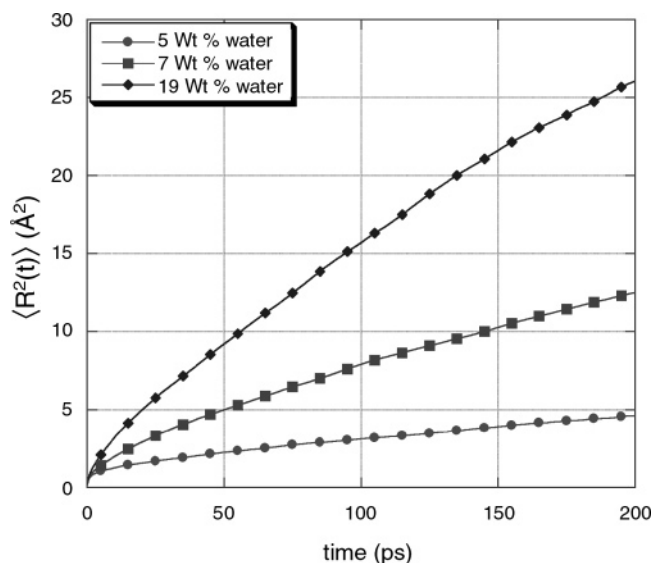


**Figure 2.** Same as Figure 1 but for Na<sup>+</sup>. The diffusion coefficients, based on data after 50 ps, are  $2.05 \times 10^{-10}$  m<sup>2</sup>/s,  $0.87 \times 10^{-10}$  m<sup>2</sup>/s, and  $0.27 \times 10^{-10}$  m<sup>2</sup>/s for 19, 7, and 5 wt % water.

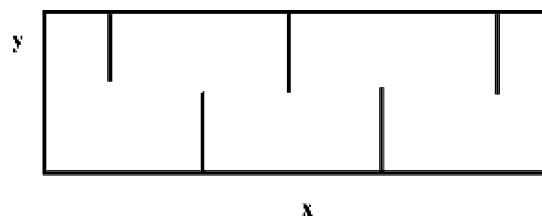


**Figure 3.** The rectangular two-dimensional box used in the simulations shown in Figure 4.

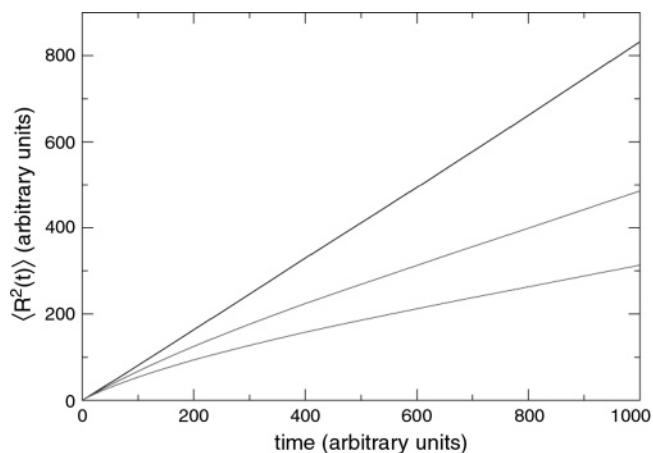


**Figure 4.** Mean squared displacement of a particle (top to bottom): freely allowed to diffuse in 2D; allowed to diffuse in a rectangular space with reflecting boundaries; and in a rectangular space with side chains pointing inward (Figure 3).

model is an infinite plane. In the second, the lattice is enclosed in a long rectangle. In the third, we added to the rectangle vertical, impenetrable obstacles (see Figure 3) to mimic trapping by the side chains. Hopping is a random Poisson process, and the rate (for hopping to any allowed site) is the same in all three simulations.

The mean-square-displacement curves for these systems are shown in Figure 4. At short times the mean-square displacements in the three systems are the same. Very few random walkers in the simulations have a chance to run into the borders or the vertical obstacles in the system; they diffuse as if these obstacles do not exist. At longer times, the walker feels the

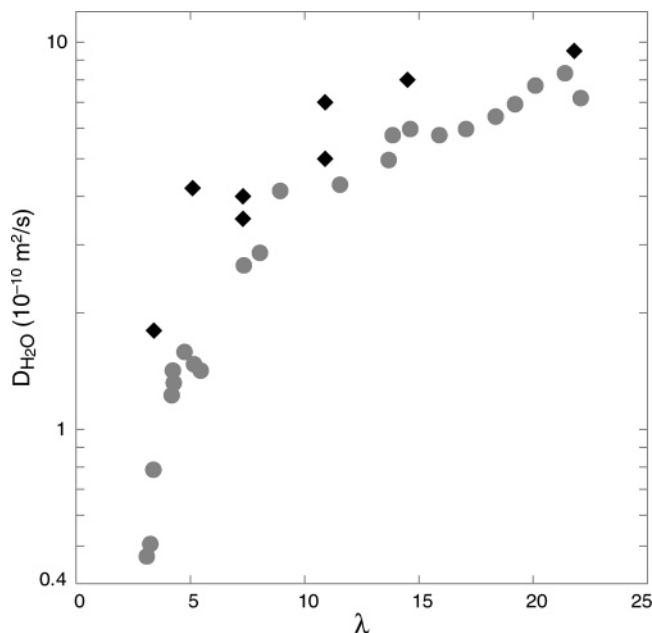


**Figure 5.** The diffusion coefficient for H<sub>2</sub>O in Nafion as a function of the number of water molecules per sulfonic group. The diamonds are the results of our calculations, based on several sets of data for both Nafion-1144, and Nafion-944, from different starting configurations. The circles are results of several NMR experiments.<sup>4</sup>

effect of the boundaries and the vertical obstacles and this slows it down.

Figures 1 and 2 show that an increase in the hydration level leads to an increase in the mobility of both H<sub>2</sub>O and Na<sup>+</sup>. Three factors are likely to be responsible for this trend. First, at low hydration levels (and hence higher ion concentrations), both Na<sup>+</sup> and H<sub>2</sub>O are more strongly influenced by the SO<sub>3</sub><sup>-</sup>, which binds effectively to both species. Second, as the wt % of water increases, the high dielectric constant of the water helps to screen charge–charge and charge–dipole interactions, making it easier for the species to move. Third, as the water volume increases there is enough water to solvate most Na<sup>+</sup> ions and this favors the dissociation of SO<sub>3</sub>Na and the hydration of the Na<sup>+</sup> ion in the center of the channel. Once dissociated the Na<sup>+</sup> ions are more mobile.

In Figure 5 we compare our predictions for the self-diffusion coefficient of water, with experimental values (using pulsed field gradient NMR) reported in a recent review by Kreuer et al.<sup>4</sup> The simulation is in good agreement with the data; however, both the experimental method<sup>23</sup> and the simulation are limited to investigation of short time and length scales.

In Figure 6 we show the self-diffusion coefficient for Na<sup>+</sup> as a function of hydration. Na<sup>+</sup> diffusion is slower than that of water, and its diffusion rate increases with hydration. Experiments on related systems<sup>24–27</sup> give  $D$  for Na<sup>+</sup> to be  $\sim 1–2 \times 10^{-10}$  m<sup>2</sup>/sec, at moderate hydration levels, similar to the values seen here. At 5 wt % hydration in Nafion-1166  $D_{\text{water}}/D_{\text{Na}} = 8$ , at 19 wt % water  $D_{\text{water}}/D_{\text{Na}} = 5$ , and at 95 wt % water  $D_{\text{water}}/D_{\text{Na}} = 2.4$ . The ion mobility increases more rapidly with the degree of hydration than the mobility of water. This is easy to understand, since at low hydration levels the Na<sup>+</sup> ions tend to coordinate with the sulfonate groups. An analysis of the terms contributing to the total energy shows that as the water content increases the average Na–Nafion electrostatic interaction diminishes. This reflects the fact that, because of solvation, the Na<sup>+</sup> move into the bulk of the hydrophilic phase. The large dipole moment of water screens the interaction of these ions

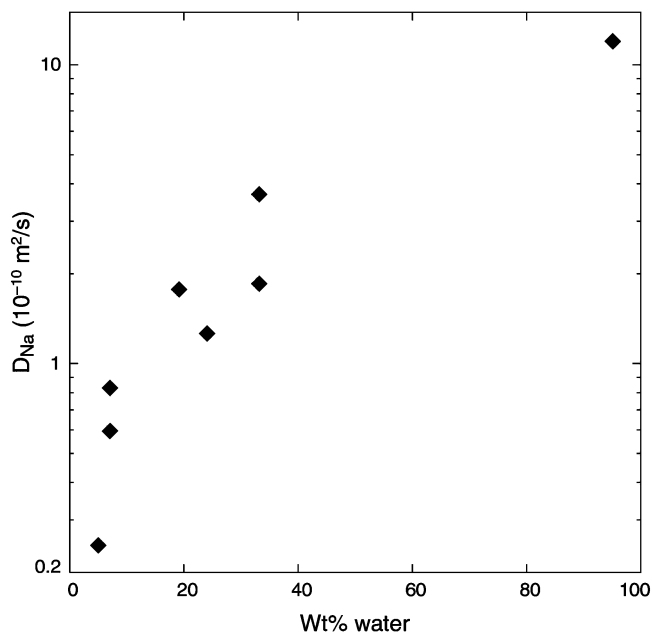


**Figure 6.** Calculated self-diffusion coefficient of Na<sup>+</sup> as a function of the hydration of the Nafion membrane.

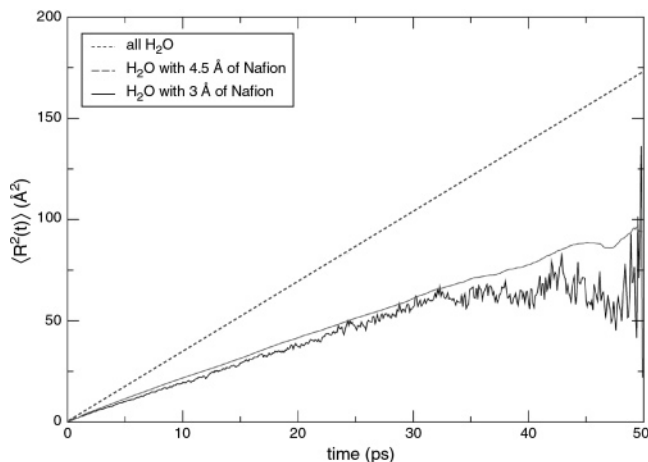


**Figure 7.** Diffusion in a very dilute Nafion salt solution (four monomers with 21 600 water molecules). Shown are mean-square displacements for all water molecules, and considering only those water molecules within 4.5 and 3  $\text{\AA}$  of the Nafion.

with the SO<sub>3</sub><sup>-</sup> charges which tend to be located along the domain walls.

**III.2. Local Diffusion of H<sub>2</sub>O.** The diffusion coefficients calculated above conceal a lot of information regarding microscopic dynamics, since all water molecules, or Na<sup>+</sup> ions, are lumped to produce one number,  $D$ . One expects that the behavior of a sodium ion located near a SO<sub>3</sub> group is rather different from that of a fully solvated ion in the middle of the channel. Different locations ought to lead to different behavior. To investigate these differences we look at the diffusive behavior of these species at different locations in the hydrophilic channel. We do this by defining a region of interest and collecting statistics for atoms or molecules that inhabit that region. Here we look at the regions around sulfonate head groups, the regions abutting the hydrophobic Teflon backbone, and those around the Na<sup>+</sup> ions.

In Figure 7 we show the mean-square displacement of H<sub>2</sub>O diffusing in a 0.0002M Nafion salt solution. By collecting statistics for only those water molecules that reside within a given distance (3 or 4.5  $\text{\AA}$ ) from the F atoms of Nafion, and

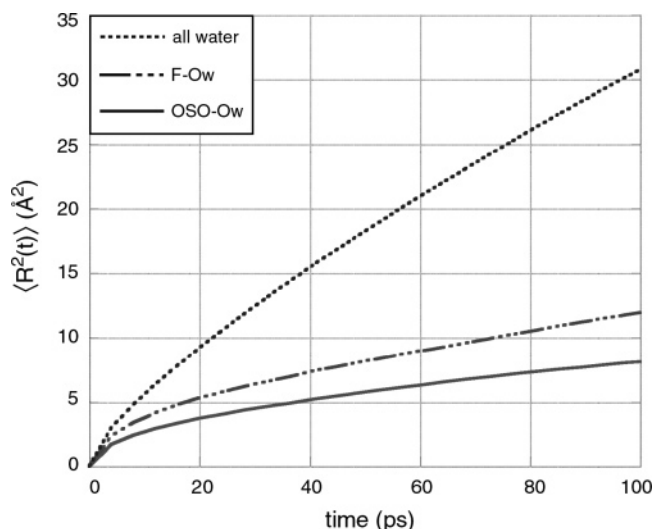


**Figure 8.** Mean-square displacements for different types of water in Nafion-1166 at 5 wt % hydration level. F-Ow and OSO-Ow refer to water molecules within 4.5 Å of the F atoms of the backbone and the O of a sulfonate group, while *all water* is the average mean-square displacement of all waters in the simulation.

comparing their statistics with bulk water, we find that the water molecules near the Teflon wall diffuse more slowly. A comparison of the slopes of the mean-square displacement curves, shows that water in the vicinity of the wall diffuses  $2/3$  as fast as bulk water.

In Figure 8 we show the mean-square displacement of water molecules near the Teflon wall, water molecules near SO<sub>3</sub> and the average displacement for the water at all locations, for Nafion-1166 at 5 wt % hydration. Water located in the neighborhood of SO<sub>3</sub> is less mobile than water molecules abutting the hydrophobic Teflon backbone. This is consistent with the observation that the average water–Nafion interaction energy decreases with increasing hydration. The water near the pore boundaries has a smaller diffusion coefficient than that found when we average over all molecules in a channel.

This also shows that the water molecules in the middle of the channel are mainly responsible for the total water diffusion. By increasing the amount of water, we increase the number of bulk-like water molecules that contribute to diffusion in Nafion. This is the main reason why water mobility increases with the level of hydration of the membrane.

To verify this interpretation, in Figure 9 we show the residence time distribution for water molecules near the domain wall, and compare it to the distribution for the water molecules located near an SO<sub>3</sub> group (still in the system with 5 wt % water). An exponential distribution is also shown for comparison (with logarithmic time bins, see Sec. II). These histograms show that the departure of a water molecule from one of these two regions is not described by a simple rate law. The most likely time for water to leave a certain region is 13 ps for water near the domain wall and 30 ps for water near a sulfonate group. This is consistent with the water-sulfonate group interaction being more attractive. These results may be compared with the departure of water from the first solvation shell of Na<sup>+</sup> in bulk water, which is a Poisson process with a time scale of  $\sim 10$  ps.<sup>28</sup>

**III.3. Local Diffusion of Na<sup>+</sup>.** In Figure 10 we plot the residence time distribution for the Na<sup>+</sup> ions near a sulfonate group. Here, we see a dramatic decrease in the most-likely residence time with increasing hydration, going from 170 ps at 7 wt % to 22 ps at 19 wt %.

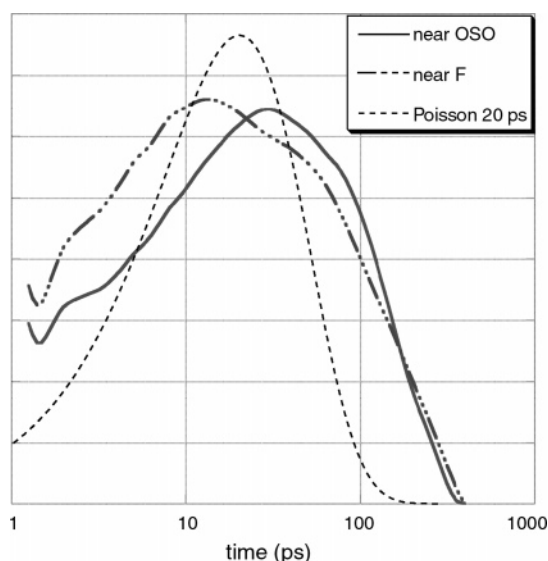


**Figure 9.** The residence time distributions  $\tau(t)$ , for water molecules within 4.5 Å of the O atoms in a sulfonate group, and within 4.5 Å of the domain wall (i.e., fluorine), in the system with 5 wt % water. The normalization ensures an exit probability of 1. The distribution of a Poisson process with a time constant of 20 ps is shown for comparison.

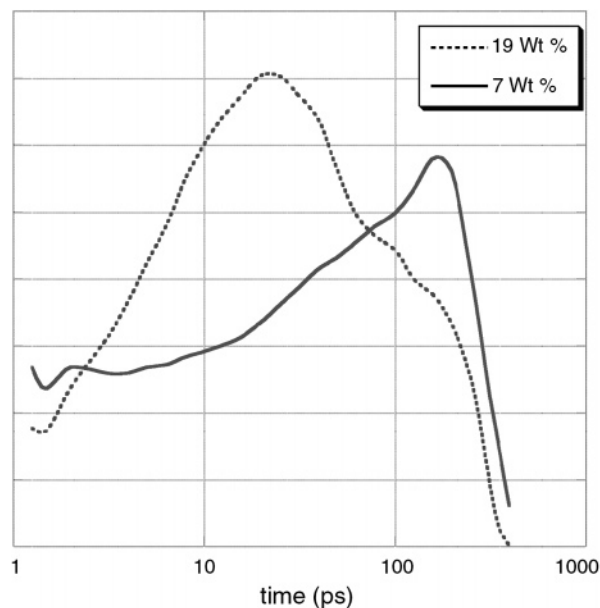


**Figure 10.** Same as Figure 9, for Na<sup>+</sup> ions within 4.5 Å of the O atoms in a sulfonate group, at 19 and 7 wt % hydration.

here. First, as the amount of water in the membrane is increased, charge–charge interactions are screened more effectively, making it easier for the Na<sup>+</sup> ions to escape from a given SO<sub>3</sub> group. Second, as the membrane swells, due to increased hydration, each Na<sup>+</sup> ion has fewer SO<sub>3</sub> groups in its immediate vicinity. The average number of SO<sub>3</sub> groups in the first solvation shell of Na<sup>+</sup> goes from 2.5 at 5 wt % to 0.5 at 19 wt %. But even at 19 wt %, 25% of all Na<sup>+</sup> ions are bound to two or more SO<sub>3</sub> groups, thus making temporary cross-links between different side-chains.

The multi-modal distributions are most likely due to the appearance of cross-linking, where Na<sup>+</sup> ions that have more than one SO<sub>3</sub> group in the first solvation shell. Those Na<sup>+</sup> ions with two or more SO<sub>3</sub> groups in their immediate vicinity will have a much harder time escaping into the bulk of the channel, and so they will exhibit longer residence times. At 5 wt % cross-linking is so prevalent that only a fraction of the Na<sup>+</sup> ions leave



within the simulation time, thus making the assessment of the residence time inaccurate. For this reason, we do not show the 5 wt % data in Figure 10. The dramatic decrease in the residence time of the Na<sup>+</sup> as a function of hydration explains why Na<sup>+</sup> diffusion is much more sensitive to the level of hydration in the membrane than is the diffusion of water.

Notice also, that although the residence times for Na<sup>+</sup> near SO<sub>3</sub><sup>-</sup>, at 7 wt % and 19 wt % water, differ by a factor of nearly 10 (Figure 10), the diffusion coefficients differ by only about a factor of 3 (Figure 2). This indicates that the diffusion is not a Poisson process consisting of hops from one SO<sub>3</sub><sup>-</sup> group to another (if that were the case then the two numbers would match), but rather there must be a significant unbound fraction of Na<sup>+</sup> which contributes most to the mobility. The shape of the residence time curves also differs qualitatively from that expected for a Poisson process (shown in Figure 9).

This apparently results from a variety of local environments of the Na<sup>+</sup> ions. If a Na<sup>+</sup> ion has only a few water molecules nearby, it is less likely that a solvent-separated ion pair will form, and the SO<sub>3</sub>Na pair remains trapped for a longer time. The rate-limiting step for breaking up this pair will be the arrival of enough waters, which is a diffusion-limited process and probably does not obey a simple rate law. A distribution closer to an exponential would have been obtained if all SO<sub>3</sub>Na pairs had identical environments; but the SO<sub>3</sub><sup>-</sup> group itself offers more than one binding site to the Na<sup>+</sup> ion, apart from the number of waters present, which produces some intrinsic spread in the Na–O residence times.

#### IV. Summary

We have calculated the diffusion coefficients of H<sub>2</sub>O and Na<sup>+</sup> in a model Na–Nafion polymer electrolyte membrane, having varying amounts of water. The hydrophilic domains, through which the ion and water transport take place, contain water, Na<sup>+</sup> ions and SO<sub>3</sub><sup>-</sup> ions tethered to side chains. These particles interact strongly and their structure and transport properties are affected substantially by the degree of hydration. At low hydration levels the hydrophilic domains form disconnected droplets in which the mobility of the water and of the ions is low. Some of the Na<sup>+</sup> ions are dissociated from SO<sub>3</sub><sup>-</sup> and are partially hydrated and the others form “bonds” with several SO<sub>3</sub><sup>-</sup> groups.

Increased hydration leads to the formation of percolating, contorted channels of irregular shape, but there is still a sharp distinction between the hydrophilic and the hydrophobic domain and it is meaningful to speak of a domain wall. The majority of the SO<sub>3</sub><sup>-</sup> groups are located in the neighborhood of these walls while the Na<sup>+</sup> tend to be located in center of the channel, where they are well hydrated. The segregation of the SO<sub>3</sub><sup>-</sup> groups near the domain walls takes place mainly because the side chains, to which they are bound, are hydrophobic.

The present results help us to understand the conditions in a real fuel cell, where the distribution of water is not uniform. The positive ions traveling from the anode to the cathode drag with them, on average, roughly two water molecules.<sup>2,29</sup> In addition, water is produced at the cathode. Since the water molecules diffuse faster than the ions, water diffusion alleviates in part the effect of the water-drag by the positive ions. Nevertheless, in a hydrogen fuel cell, the anodic region has lower water loading and this may limit the mobility of the

positive ions. A low hydration level in any region of the membrane will lower ion mobility; thus water management is an important factor in controlling the performance of the membrane.

Our results largely agree with experimental measurements in related systems. The H<sub>2</sub>O and Na<sup>+</sup> diffusion coefficients are slower in the Nafion channels than in bulk water by about a factor of 10. This is due in part to the large concentration of ions and the confinement caused by small channel size. Since the system is inhomogeneous, diffusion is a superposition of contributions from different local environments. Separation of these shows that the mobility is mainly due to those ions and waters (if any) that are *not* trapped by either the hydrophobic walls, or by temporarily forming SO<sub>3</sub>Na groups. As the amount of water is reduced, the Na<sup>+</sup> diffusion slows down more than does H<sub>2</sub>O diffusion because of the additional tendency of Na<sup>+</sup> to be trapped by SO<sub>3</sub><sup>-</sup> groups.

**Acknowledgment.** This work was supported by a MURI grant from the Army Research Office. We had useful discussions with Greg Voth, Brad Chmelka, and Steve Buratto.

#### References and Notes

- (1) Kreuer, K. D. *J. Membrane Sci.* **2001**, *285*, 29.
- (2) Alberti, G.; Casciola, M. *Annu. Rev. Mater. Res.* **2003**, *33*, 129.
- (3) Mauritz, K. A.; Moore, R. B. *Chem. Rev.* **2004**, *104*, 4535.
- (4) Kreuer, K. D.; Paddison, S. J.; Spohr, E.; Schuster, M. *Chem. Rev.* **2004**, *104*, 4637.
- (5) Blake, N. P.; Petersen, M. K.; Voth, G. A.; Metiu, H. *J. Phys. Chem. B* **2005**, *109*, 24244.
- (6) Paul, R.; Paddison, S. J. *J. Chem. Phys.* **2005**, *123*, 224704.
- (7) Paddison, S. J.; Elliott, J. A. *Phys. Chem. Chem. Phys.* **2006**, *8*, 2093.
- (8) Elliott, J. A.; Hanna, S.; Elliott, A. M. S.; Cooley, G. E. *Phys. Chem. Chem. Phys.* **1999**, *1*, 4845.
- (9) Vishnyakov, A.; Neimark, A. V. *J. Phys. Chem. B* **2000**, *104*, 4471.
- (10) Vishnyakov, A.; Neimark, A. V. *J. Phys. Chem. B* **2001**, *105*, 7830.
- (11) Vishnyakov, A.; Neimark, A. V. *J. Phys. Chem. B* **2001**, *105*, 9586.
- (12) Li, T.; Wlaschin, A.; Balbuena, P. B. *Ind. Eng. Chem. Res.* **2001**, *40*, 4789.
- (13) Paddison, S. J. *Annu. Rev. Mater. Res.* **2003**, *33*, 289.
- (14) Jang, S. S.; Molinero, V.; Cagin, T.; Goddard, W. A. *J. Phys. Chem. B* **2004**, *108*, 3149.
- (15) Tuckerman, M. E.; Laasonen, K.; Sprik, M.; Parrinello, M. *J. Phys.: Condens. Matter* **1994**, *6*, A93.
- (16) Lobaugh, J.; Voth, G. A. *J. Chem. Phys.* **1996**, *104*, 2056.
- (17) Day, T. J. F.; Soudackov, A. V.; Cuma, M.; Schmitt, U. W.; Voth, G. A. *J. Chem. Phys.* **2002**, *117*, 5839.
- (18) Kornyshev, A. A.; Kuznetsov, A. M.; Spohr, E.; Ulstrup, J. *J. Phys. Chem. B* **2003**, *107*, 3351.
- (19) Petersen, M. K.; Wang, F.; Blake, N. P.; Metiu, H.; Voth, G. A. *J. Phys. Chem. B* **2005**, *109*, 3727.
- (20) Cieplak, P.; Caldwell, J.; Kollman, P. *J. Comp. Chem.* **2001**, *22*, 1048.
- (21) Jorgensen, W. L.; Chandrasekhar, J.; Madura, J. D.; Impey, R. W.; Klein, M. L. *J. Chem. Phys.* **1983**, *79*, 926.
- (22) Ryckaert, J. P.; Ciccotti, G.; Berendsen, H. J. C. *J. Comp. Phys.* **1977**, *23*, 327.
- (23) Gong, X.; Bandis, A.; Tao, A.; Meresi, G.; Wang, Y.; Inglefield, P. T.; Jones, A. A.; Wen, W.-Y. *Polymer* **2001**, *42*, 6485.
- (24) Okada, T.; Møller-Holst, S.; Gorseth, O.; Kjelstrup, S. *J. Electroanal. Chem.* **1998**, *442*, 137.
- (25) Rollet, A.-L.; Simonin, J.-P.; Turq, P. *Phys. Chem. Chem. Phys.* **2000**, *2*, 1029.
- (26) Goswami, A.; Acharya, A.; Pandey, A. K. *J. Phys. Chem. B* **2001**, *105*, 9196.
- (27) Rollet, A.-L.; Diat, O.; Gebel, G. *J. Phys. Chem. B* **2004**, *108*, 1130.
- (28) Ohtaki, H.; Radnai, T. *Chem. Rev.* **1993**, *93*, 1157.
- (29) Saito, S.; Arimura, N.; Hayamizu, K.; Okada, T. *J. Phys. Chem. B* **2004**, *108*, 16064.